FED-Vol. 228, Gas-Particle Flows
ASME 1995

EFFECTS OF PARTICLE PROPERTIES ON THE STRUCTURE OF CLUSTERS

Toshitsugu Tanaka, Shigeru Yonemura and Yutaka Tsuji
Department of Mechanical Engineering
Osaka University
Suita, Osaka
Japan

ABSTRACT

Effects of physical properties of particles on the structure of particle clusters are studied numerically. The numerical simulations were made on two-dimensional upward gas-solid flows in a rectangular domain with periodic boundaries. Flow fields of gas and solid are solved simultaneously taking the interaction between both phases into consideration. Flows of the solid phase are obtained by calculating individual particle motions, *i.e.* by the Lagrangian method, while gas flows are obtained by solving the equations of inviscid fluid. The Direct Simulation Monte Carlo (DSMC) method is used to take account of particle-to-particle collisions. The following results are obtained. The spatial structure of a cluster predicted is like a strand. There are two typical types of clusters, a V-shaped cluster and an inverse V-shaped one. These patterns are consistent with previous experiments. The size of cluster increases with increasing the particle size. The predicted range of cluster size agreed with the experiments by Horio and Kuroki (1994).

1. INTRODUCTION

Upward gas-solid flows in a vertical pipe or duct show various flow patterns according to the gas velocity and the solid loading. The flow is stable and particle distribution is nearly uniform at high gas velocity. When the gas velocity is reduced, the flow becomes unstable and inhomogeneous. Such an unstable flow pattern is observed in fast fluidized beds and in dense phase pneumatic conveyors. Many studies on such flows have been done in the interest of these industrial applications.

One of the significant features of this kind of unstable flow is formation of clusters which are remarkably dense clouds in the flows. Generally a cluster has large spatial scale compared with the individual particle, and shows complicated behavior, therefore the effect of particles on flow structure in the unstable flows is quite different from that in the dilute flows. It is important to know the structure and the behavior of clusters for understanding the transport phenomena between gas and particles.

Numerical simulation is a useful method to study this flow. Because the presence of particles does not make the flow fields less accessible, and it is easy to change parameters. Lagrangian approach is widely used to predict particles motion in dilute flows in which particle-to-particle interaction is negligible. In order to deal with flows of medium particle concentration the particle-to-particle interaction or the particle-to-particle collision must be considered. Yonemura et al. (1993) succeeded in predicting the unstable flows with clusters numerically by applying the direct simulation Monte Carlo (DSMC) method (Bird, 1976), which is widely used for solving rarefied gas flows with inter-molecular collisions, to the calculation of the particle motions. Their result shows an unstable motion of clusters and a typical V-shaped cluster. Horio and Kuroki (1994) observed cluster patterns in a circulating fluidized bed by using a laser sheet visualization technique, and found that the similar paraboloidal cluster is a typical one.

The present paper deals with the effect of physical properties of particles on the structure of the clusters predicted by the numerical simulation similar to that by Yonemura et al. (1993). Periodic boundaries are introduced to improve spatial resolution and to see a fully developed flow in detail.

2. BASIC EQUATIONS AND NUMERICAL METHOD

2.1 Particle Motion

2.1.1 Treatment of Particle Motion. The treatment of particle motion is basically the same as our previous paper (Yonemura et al., 1993), so that only the outline is

shown here. The flows studied in the present paper are two-dimensional. It means that macroscopic flows of both phases are two-dimensional, but individual particle motion is not restricted to two-dimensional one like as the motion of molecules in two-dimensional gas flow. The Lagrangian approach is applied to the calculation of particle motions. It is assumed that particles interact only through particle-to-particle collisions. Consequently, motions are described with the equation of motion and the equation of impulsive motion for a particle.

2.1.2 DSMC Method. Interaction between particles is described with the impulsive equations of motion in which collision with another particle is assumed to be instantaneous. From this aspect the motion of the particle is similar to that of a molecule in rarefied gas. The DSMC method is an efficient method to deal with rarefied gas flows with inter-molecular collisions. The DSMC method has already been applied to calculate particle motion in gas-solid flows by Kitron et al. (1990), Tanaka et al. (1991) and Yonemura et al. (1993).

According to the DSMC method the calculation of particle motion was carried out by repeating the following procedure:

(1) First, the motions of all simulated particles in a time step Δt are calculated by the equations of motion, which is shown in the following section, without regard for inter particle collisions.

(2) Second, particle-to-particle collisions in Δt are calculated. Whether a simulated particle collides with another particle is determined by the Monte-Carlo method. If a simulated particle comes into collision with another particle, the post collision velocity is calculated by the impulsive equations of motion,*i.e.* Eq.(9) and Eq.(10) in section 2.1.4. The Monte-Carlo method is used again to give the configuration of the collision. The particle velocities are replaced by the post collision velocities, but without changing their positions.

There are several schemes to treat particle-to-particle collisions. In the present simulation the modified Nanbu method (Illner and Neunzert, 1987) is used. A particle-to-particle collision is given based on the collision probability. The collision probability of particle i in $\Delta t$is given by,

$$P_i = \sum_{j=1}^{N} P_{ij}, \tag{1}$$

where N is the number of simulated particles in the cell and P_{ij}, the probability of collision between particle i and particle $j$contained in the cell.

It must be noticed that each simulated particle represents many physical particles. Therefore, P_{ij} is not a collision probability between a single particle i and a single particle j but that for a physical particle represented by these simulated particles. Assuming the particles are spheres with a uniform diameter d, P_{ij} is given by,

$$P_{ij} = \frac{n}{N}\pi d^2 g_{ij}\Delta t, \tag{2}$$

where n is the number density of the particles at the corresponding position in the real flow, and g_{ij} is the magnitude of relative velocity between the both particles.

The modified Nanbu method uses a random number for determining the occurrence of particle-to-particle collision and for finding a collision partner. If the particle i collides with the particle k, the velocity of particle$i$ s replaced by velocity after the collision according to the impulsive equation of motion.

2.1.3 Equation of Motion for a Particle. The equation of translational motion for a particle is

$$m\frac{d\boldsymbol{v}}{dt} = -\frac{\pi}{6}d_p^3\nabla p + \boldsymbol{F}_f + m\boldsymbol{g}_G, \tag{3}$$

where m is the mass of the particle, $\boldsymbol{v}$, particle velocity, $\boldsymbol{g}_G$ is the gravitational acceleration, and $\boldsymbol{F}_f$ is the fluid force exerted on the particle. The first term in the right side of Eq.(3) represents the force caused by the pressure gradient, which was neglected in our previous paper (Yonemura et al., 1993). However, it was found that this term affects the slip velocity between particles and gas for high solid loading, so that it is considered here.

The fluid force $\boldsymbol{F}_f$ is assumed to be given by

$$\boldsymbol{F}_f = \frac{1}{2}\rho_f|\boldsymbol{u}_R|A\left(C_D\boldsymbol{u}_R + C_{LR}\frac{bmu_R\times\boldsymbol{\omega}_R}{|\boldsymbol{\omega}_R|}\right) + \boldsymbol{f}_{LG}, \tag{4}$$

where A is the projected area of the particle, ρ_f, fluid density, $\boldsymbol{u}_R$, gas velocity relative to the particle, and $\boldsymbol{\omega}_R$ is the rotational velocity of the particle relative to the fluid;

$$bm\omega_R = bm\omega - \frac{1}{2}\nabla\times\boldsymbol{u}, \tag{5}$$

where $bm\omega$ is the rotational velocity of a particle.

The first term in the right side of Eq.(4) represents the drag force, the second term, the Magnus lift force, and $\boldsymbol{f}_{LG}$, the lift force due to velocity gradient. The standard drag coefficient for a single sphere in a uniform flow was used as C_D (Morsi and Alexander, 1972). The following expression was assumed for C_L (Maccoll, 1928; Davis, 1949; Barkla and Auchterlonie, 1971; Tanaka et al., 1990).

$$C_L = \min[\,0.5\ ,\ 0.25\frac{d\omega}{|\boldsymbol{u}_R|}\,]. \tag{6}$$

where min[a,b] is defined as a function which gives the minimum value between a and b.

For the lift force $\boldsymbol{F}_{LG}$ due to velocity gradient, Saffman's theoretical result (1965) was used. Only the horizontal component of $\boldsymbol{F}_{LG}$ was considered here.

$$F_{LGy} = 1.62u_{Rz}d^2\sqrt{\rho_f\mu}\frac{du_{Rz}/dy}{\sqrt{|du_{Rz}/dy|}} \tag{7}$$

where u_{Rz} is the z component of $\boldsymbol{u}_R$.

The equation of rotational motion for a particle is given by

$$I\frac{d\boldsymbol{\omega}}{dt} = -C_T\frac{1}{2}\rho\frac{d}{2}^5|\boldsymbol{\omega}_R|\boldsymbol{\omega}_R, \tag{8}$$

where I is the moment of particle inertia. The right side of equation(8) is the viscous torque against particle rotation, which is theoretically obtained by Takagi (1977) and Dennis et al. (1980).C_T is the non-dimensional coefficient which depends on $Re_R = |\omega_R| d^2/(4\nu)$.

2.1.4 Equation of Impulsive Motion for a Particle.

Assuming that the relaxation time of particles to fluid forces is long compared with the duration of particle interaction, fluid forces due to interactions between particles are neglected. The equations of impulsive motion for a particle are given as follows,

$$\boldsymbol{v}^* = \boldsymbol{v} + \boldsymbol{J}/m, \tag{9}$$

$$\boldsymbol{\omega}^* = \boldsymbol{\omega} + \frac{d}{2I}\boldsymbol{n} \times \boldsymbol{J}, \tag{10}$$

where $\boldsymbol{n}$ is the normal unit vector directed from the particle to outside on the contact point, and $\boldsymbol{J}$ is the impulsive force on the particle. Post-collision quantities are indicated by an asterisk.

The following assumptions are introduced to calculate the impulsive force $\boldsymbol{J}$.

(1) The particle is spherical, and deformation of the particle is negligible.
(2) The coefficient of restitution e is constant.
(3) The tangential impulsive force during the slip motion is given by the Coulomb's friction law.
(4) Slip between particles does not occur again after the initial slip stops.

According to these assumptions $\boldsymbol{J}$ is given as follows (Tanaka and Tsuji, 1991).

$$\boldsymbol{J} = J_n \boldsymbol{n} + J_t \boldsymbol{t} \tag{11}$$

$$J_n = \frac{1}{2}(1+e) m \boldsymbol{n} \cdot \boldsymbol{g} \tag{12}$$

$$J_t = \min[\, -\mu_F J_n \,,\, \frac{1}{7} m |\boldsymbol{g}_F| \,] \tag{13}$$

In the above equation, $\boldsymbol{t}$ is the tangential unit vector directed to $\boldsymbol{g}_F$ which is the slip velocity of the collision partner, $\boldsymbol{g}$ is the relative velocity of the collision partner to the particle, e is the coefficient of restitution, and μ_F is the coefficient of kinetic friction.

2.2 Calculation of Fluid Flow

The fluid is assumed to be incompressible and inviscid except the fluid force on particles. The fluid flow field is described with "local mean variables" which is defined as a locally averaged value in the volume occupied by the fluid (Anderson & Jackson, 1967). The equation of continuity and the equation of motion used here are as follows;

$$\frac{\partial \varepsilon}{\partial t} + \nabla \cdot (\varepsilon \boldsymbol{u}) = 0, \tag{14}$$

$$\varepsilon \frac{D}{Dt}(\boldsymbol{u}) = -\frac{\varepsilon}{\rho}\nabla p + \frac{\boldsymbol{F}_p}{\rho}, \tag{15}$$

where ε is the void fraction, p, pressure, and $\boldsymbol{F}_p$, the force exerted on the fluid by particles contained in a unit volume.

These equations were solved by the SIMPLE method (Patankar, 1980). The calculation domain is divided into rectangular cells of dimensions $\Delta y_f \times \Delta z_f$. ε is given explicitly by

$$\varepsilon = 1 - \frac{\alpha N_f V_p}{\Delta y_f \Delta z_f}, \tag{16}$$

where N_f is the number of simulated particles contained in the fluid calculation cell, V_p, the volume of a particle, and α, the ratio of the concentration of "physical" particles to that of simulated particles. $\boldsymbol{F}_p$ is the reaction of fluid forces acting on particles:

$$\boldsymbol{F}_p = -\frac{\alpha}{\Delta y_f \Delta z_f} \sum_{i=1}^{N_f} \boldsymbol{F}_{fi}. \tag{17}$$

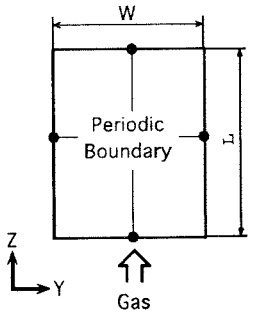

Fig 1. Calculation domain

Table 1. Calculation conditions

Gas density ρ_f [kg/m^3]	1.205		
Viscosity μ [Pa · s]	1.81×10^{-5}		
Particle diameter d [μ m]	61.3	200	500
Superficial gas velocity [m/s]	0.6	2.0	5.0
Particle density ρ_p [kg/m^3]	1780		
Mean particle velocity at the initial condition V_I [m/s]	0.0		
Coefficient of restitution between particles e_p	0.9		
Coefficient of friction between particles μ_{Fp}	0		

3. RESULTS AND DISCUSSION

3.1 Conditions of Simulation

The calculation domain is rectangular one with periodic boundaries as shown in Fig.1. Table 1 shows the principal conditions. The physical properties of the gas are the same as those of the air at atmospheric pressure and room temperature. Particles are assumed to be rigid spheres. Three kinds of particle sizes, d =61.3, 200, 500 [μm], are used. The terminal velocities of these particles in the specified atmosphere are 0.188, 1.09 and 3.00 [m/s], respectively. The superficial gas velocity is kept constant during each calculation. However, the magnitude of the superficial gas velocity dose not affect the phenomenon observed in the domain except for the vertical components of mean velocities, because there is no solid boundary.

The calculation region is divided into 80×80 rectangular cells for both phases. The size of the calculation domain was

changed according to the particle size, because the spatial scale of clusters obtained in the present simulation largely depends on the particle size. The total number of the simulated particles is 640,000. Consequently, the average number of particles contained in a cell is 100. The total number of the simulated particles dose not change during each calculation, as all boundaries are periodical ones.

Uniform flow condition is given as the initial condition. The locally averaged particle velocity is uniform, but fluctuation velocity component is given to each simulation particle. The time step was chosen as to be smaller than the local mean free time of particles.

3.2 Flow Pattern and the Structure of Clusters

For all the calculation conditions, nonuniformities appeared in distributions of particles. In the cases of high solid volume fraction such nonuniformities developed to dense clusters, and the flows became unstable. Fig.2 shows the distributions of solid volume fraction varying with time. It is observed that nonuniformities or clouds whose spatial scales are comparatively small appear first. These small clouds grow to dense clusters. The spatial structure of the developed cluster is like a bent strand. These clusters tend to form a complicated network. These clusters show unstable behavior. Some clusters vanish, and some clusters appear. Several clusters coalesce into one dense cluster, and a cluster is broken into several clusters.

The structure of the individual cluster is not simple, but there are some typical patterns. One typical pattern is a V-shaped cluster, and the other is an inverse V-shaped cluster.

The V-shaped cluster is also observed in our previous simulation (Yonemura et al., 1993), and the similar cluster is observed in the experiments by Horio and Kuroki (1994). Horio and Kuroki visualized clusters in a circulating fluidized bed by using the laser sheet visualization technique. They found that the average shape of a cluster in a vertical cross section is a parabola, *i.e.* a V-shaped one, and that the three-dimensional structure of such a cluster is a paraboloid. Horio and Kuroki do not mention about an inverse V-shaped cluster.

Takeuchi *et al.* (1994) observed the behavior of clusters in a riser of circulating fluidized bed. The measurement was made by using a high speed video and an optical measuring system. They found that the strand type cluster is a typical one especially in the core region of a riser. They observed the inverse V-shaped clusters.

The spatial structure of clusters predicted by the present simulation is consistent with the previous experiments as a whole.

Let us go into the flow field around these types of clusters to see their characteristics further. Fig.3 shows a snapshot of distribution of the particle concentration and the locally averaged velocities of the particles and the gas. Several V-shaped clusters and inverse V-shaped clusters are observed in this figure. Generally, the V-shaped clusters have downward or relatively small upward velocity, while the inverse V-shaped clusters relatively large upward velocity. This characteristic of the V-shaped clusters is natural, because dense clusters tend to reduce the upward flow. The gas flow around such a cluster has higher upward velocity than that of the cluster, and blows the tails of the cluster upward. Consequently, the cluster becomes V-shaped one. On the other hand, relatively thin part of a cluster network is sometimes blown upward, and forms the inversed V-shaped cluster. Therefore, the inverse V-shaped clusters tend to be formed in the downstream of a gap between low velocity clusters.

3.3 Effect of the Particle Size on the Cluster Size

Fig.4 shows the effect of the particle size on the cluster structure. The solid volume fraction, ε, is kept constant for all these cases. As the ratio of scale reduction is common, it is easy to compare the size of cluster. It is remarkable that the spatial scale of the cluster largely depends on the particle size. The size of the cluster increases with increasing the particle size.

The sizes of the V-shaped clusters were obtained following the procedure by Horio and Kuroki (1994). They defined the size of the V-shaped cluster d_{cl} by its width. Fig.5 shows the relation between the cluster size d_{cl} and the mean solid volume fraction. The number of clusters observed in the present simulations is not so large. Therefore, only the rough ranges of size distribution are given in this figure.

The diameter and the density of the 61.3 μm particle in the present simulation are the same as those by Horio and Kuroki (1994). So it is possible to compare the present results with their experiment directly. The range of cluster size for d_p =61.3[μm] agreed well with the experiments. However, there is a difference in dependence on the solid volume fraction. The measured cluster size decreases with increasing the solid volume fraction, while the calculated cluster size for d_p =61.3 [μm] does not change in the region of low solid loading. In the region of high solid loading the tendency is opposite to the experiment. For the case of d_p =200[μm], the dependence of the cluster size on the solid volume fraction agrees with the experiment.

The correlation between the size of clusters and the particle relaxation distance is investigated. Fig.6 shows the relation between the cluster size d_{cl} and the particle relaxation distance l_R, which is defined by

$$l_R = v_t \tau_R, \tag{18}$$

where v_t is the terminal velocity of the particle, and τ_R is the particle relaxation time given by

$$\tau_R = \frac{v_t}{g}. \tag{19}$$

Particles shot into a cluster are scattered by particle-to-particle collisions. This scattering motion of particles is dissipated by inelastic collisions and the fluid drag. Therefore, the larger the particle relaxation distance, the wider the particle spreading. Fig.6 shows the relation between the cluster size d_{cl} and the particle relaxation distance l_R. The plotted range for each particle involves all data in Fig.5. This figure shows that the size of cluster is nearly proportional to the 0.5th powers of the particle relaxation distance.

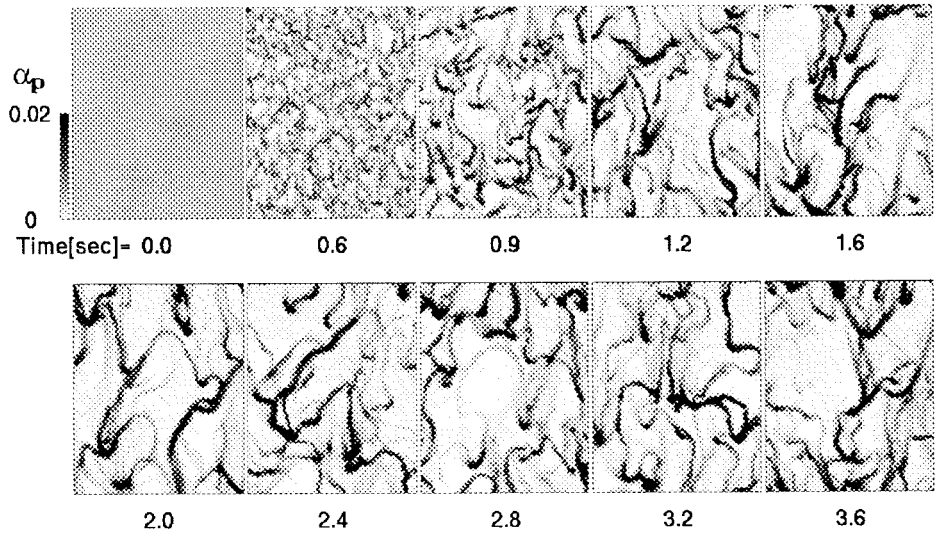

Fig 2. Distributions of solid volume fraction varying with time (d_p =61.3 μm, $\bar{\alpha_p}$ = 0.004, W = 0.2 m, L=0.25 m)

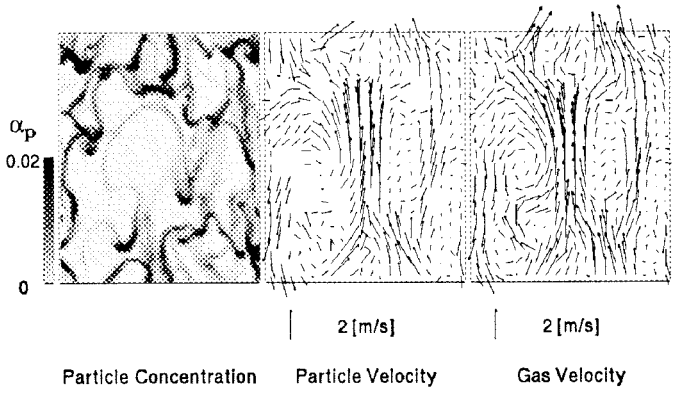

Fig 3. Flow field around clusters (d_p =61.3 μm, , W = 0.2 m, L=0.25 m)

4. Conclusion

The effects of physical property of particles on the structure of clusters are studied by a numerical simulation. The results are summarized as follows.

(1) The spatial structure of the developed cluster obtained is like a strand. These strand type clusters tend to make a network.

(2) Two typical structures are observed. One is a V-shaped cluster, and the other is an inverse V-shaped cluster. These patterns of clusters are consistent with the previous experiments.

(3) The size of cluster increases with increasing the particle size. The cluster size for the 61.3 μm particle that predicted by the present simulation agreed with the experiments by Horio and Kuroki (1994).

REFERENCES

Bird, G. A., 1976, "*Molecular Gas Dynamics*," Oxford Univ. Press, p. 118.

Barkla, H. M. and Auchterlonie, 1971, "The Magnus or Robins Effect on Rotation Spheres," *J. Fluid Mech.*, Vol. 47, Part 3, pp. 437-447.

Davis, J. M., 1949, "The Aerodynamics of Golf Balls," *J. Appl. Phys.*, Vol. 20, No. 9, pp. 821-828.

Dennis, S. C. R., Singh, S. N. and Ingham, D. B., 1980, "The Steady Flow due to a Rotating Sphere at Low and Moderate Reynolds Number," *J. Fluid Mech.*, Vol. 101, pp. 257-270.

Horio, M. and Kuroki, H., 1994, *Chem. Eng. Sci.*, Vol.49, N0.15, pp. 2413-.

Illner, R. and Neunzert, H., 1987, "On simulation methods for the Boltzmann equation," *Transport Theory and Statistical Physics*, Vol.16, pp. 141-154.

Kitron, A., Elperin, T., and Tamir, A., 1990, "Monte

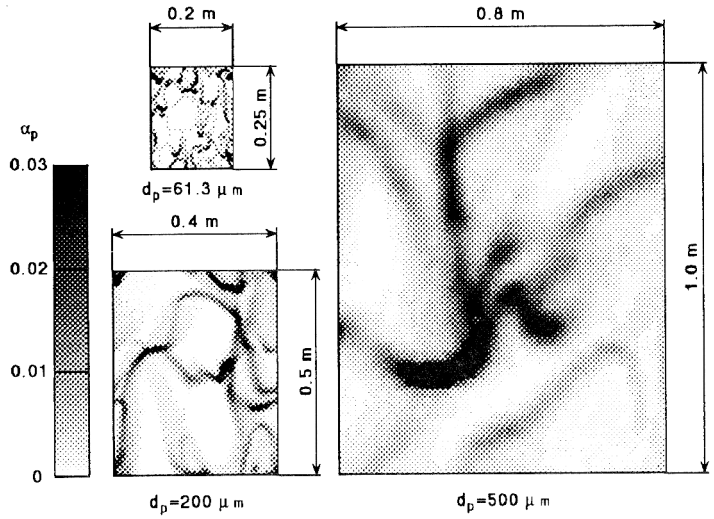

Fig 4. Effect of the particle diameter on the cluster structure ($\bar{\alpha_p} = 0.004$)

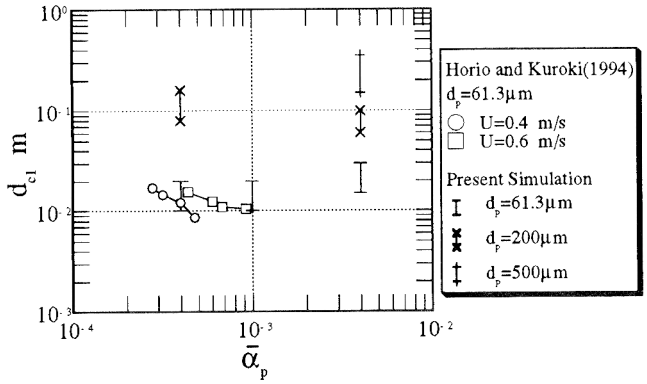

Fig 5. Effect of the mean solid volume fraction on the cluster size

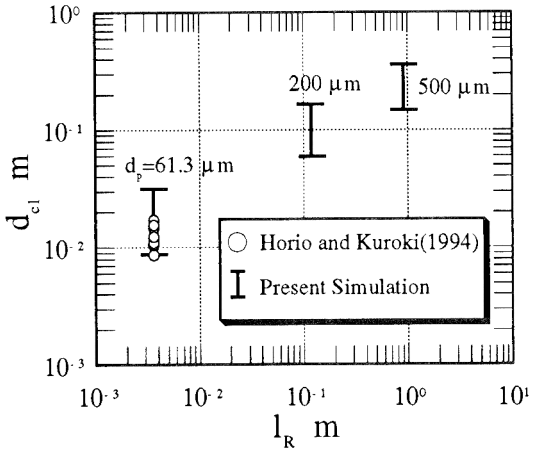

Fig 6. Relation between the cluster size and the relaxation distance

Carlo Simulation of Gas-Solids Suspension Flows in Impinging Streams Reactors," *Int. J. Multiphase Flow*, Vol.16, No. 1, pp. 1-17.

Maccoll, J.W., 1928, "Aerodynamics of a Spinning Sphere," *J. Roy. Aero. Sci.*, Vol. 32, pp. 777-798.

Morsi, S. A. and Alexander, A. J., 1972, "An Investigation of Particle Trajectories in Two-Phase Flow System," *J. Fluid Mech.*, Vol. 55, Part.2, pp. 193-208.

Patankar, S.V., 1980 *Numerical Heat Transfer and Fluid Flow*, Hemisphere Publishing Corporation.

Saffman, P. G., 1965, "The Lift on a Small Sphere in a Slow Shear Flow,", *J. Fluid Mech.*, Vol. 22, Part 2, pp. 385-400; Corrigendum 1968, Vol. 31, p. 624.

Takagi,H., 1977, "Viscous Flow Induced by Slow Rotation of a Sphere," *J. Phys. Soc. Japan*, Vol. 42, pp. 319-325.

Tanaka, T., Yamagata, K. and Tsuji, Y., 1990, "Experiment of Fluid Forces on a Rotating Sphere and Spheroid," *Proc. Second KSME-JSME Fluids Engineering Conf.*, Seoul, Korea, Vol.1, pp. 366-369.

Tanaka, T. and Tsuji, Y., 1991, "Numerical Simulation of Gas-Solid Two-Phase Flow in a Vertical Pipe: On the Effect of Inter Particle Collision," *Gas-Solid Flows - 1991*, ASME/FED Vol.121, pp. 123-128.

Tanaka, T., Kiribayashi, K. and Tsuji, Y., 1991, "Monte Carlo Simulation of Gas-Solid Flow in Vertical Pipe or Channel," *Proc. Int. Conf. on Multiphase Flows '91-Tsukuba*, Tsukuba, Japan, Vol.2, pp. 439-442.

Yonemura, S., Tanaka, T. and Tsuji, Y., 1993, "Cluster Formation in Gas-Solid Flow Predicted by the DSMC Method" *Gas-Solid Flows - 1993*, ASME/FED Vol.166, pp. 303-309.